AI-Enabled Fusion of Electrocardiograph and Demographics for Prediction of Acute Kidney Injury Onset

Vasundhara Damodaran[‡], Jose Sanchez[‡], Tushar Gupta[‡], Phaneendra Bikkina[†], Esko Mikkola[†], Abdul-Muhsin Haidar*, Imon Banerjee*, and Arindam Sanyal[‡]

*Mayo Clinic, Phoenix, AZ, USA.

[†]Alphacore Inc., AZ USA.

[†]School of Electrical, Computer and Energy Engineering, Arizona State University, AZ, USA. Email: vdamoda2@asu.edu

Abstract-Acute kidney injury (AKI) is a commonly encountered medical problem that is associated with poor health outcomes in AKI survivors, including increased mortality and re-admission to the hospital. Despite their high-risk status, only a small fraction (< 10%) of patients receive specialized nephrologist follow-up after AKI event. To address the gap in care for AKI patients, this work proposes an artificial intelligence (AI) based fusion technique that combines patient's single-lead electrocardiograph (ECG) and demographics to predict AKI recurrence 3-7 days before onset. The ECG data is analyzed with an on-chip reservoir-computer (RC) prototyped in 28nm CMOS process to create a compressed representation for predicting AKI onset from ECG. After fusion with demographics, the proposed technique is able to predict AKI recurrence 3-7 days before onset with 75.8% accuracy when evaluated on a retrospective patient dataset collected from Mayo Clinic Enterprise.

Index Terms—Machine learning, electrocardiograph, acute kidney injury, reservoir-computer and sensor fusion

I. Introduction

Acute kidney injury (AKI) is a commonly encountered medical problem associated with poor health outcomes in AKI survivors, including increased mortality and re-admission to the hospital. A recent study of AKI survivors [1] showed 18% hospital re-admission rate and 8% mortality within 30 days after discharge, with recurring AKI being the most common factor for re-admission. Despite the high re-admission and mortality rates, a majority of AKI patients decline enrollment to specialized renal follow-up care for reasons including hospital fatigue and long travel times [1].

This work proposes an at-home monitoring solution for AKI patients that uses artificial intelligence (AI) to predict AKI recurrence within a 3-7 days window prior to onset of AKI event. The proposed technique combines patient's electrocardiograph (ECG) and demographic information (age, race and gender) to predict AKI recurrence. Fig. 1 presents an overview of the proposed AKI recurrence prediction technique. A reservoir-computer (RC) is used to analyze single-lead ECG samples locally and encode into a compressed and dense representation. Single-lead ECG signal captures electrolyte abnormalities in severe case of AKI. A neural network analyzes the dense representation from the RC to predict AKI onset and is referred to as ECG model in Fig. 1. Similarly, a neural network predicts

AKI onset from the demographic information obtained from the patient's electronic medical record (EMR) and is referred to as EMR model in Fig. 1. Finally, a third neural network combines prediction scores from the ECG and EMR models to predict AKI onset with higher accuracy than either the ECG or EMR models individually. The RC is implemented as a test-chip fabricated in 28nm CMOS process, while the ECG, EMR and fusion AI models are realized in software with the eventual goal of running these AI models natively on a smartphone. Encoding the ECG data using in-sensor RC is expected to extend battery lifetime of ECG sensor by reducing radio-frequency (RF) transmission. This is plausible since RC can extract key information from sparse ECG signal using a small number of neurons due to hyper-dimensionality of RC [2].

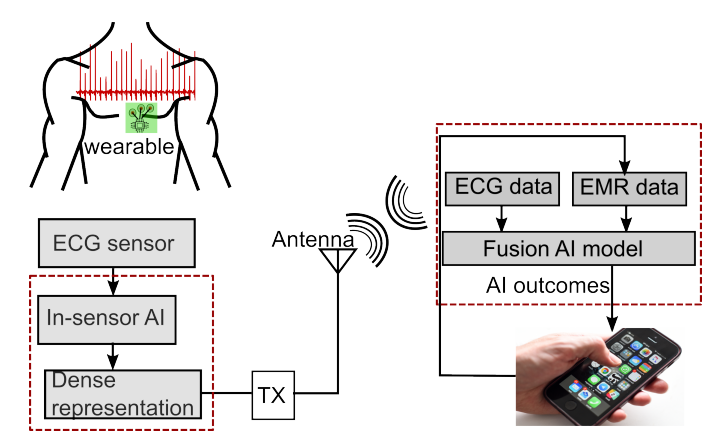


Fig. 1: Overview of the proposed technique for predicting AKI onset through AI-enabled fusion of ECG and demographic information with the contributions of this paper enclosed within red, dotted boxes

The rest of this paper is organized as follows: Section II introduces the retrospective dataset that is used in this work, Section III presents the circuit architectures and AI-based fusion model, Section IV presents measurement results on a 28nm test-chip, and finally Section V brings up the conclusion.

II. DATASET

Retrospective patient data with more than 30000 samples was collected from Mayo Clinic Enterprise. The patient data was filtered to ensure that an ECG sample was collected from the patient within 3-7 days prior to diagnosis (AKI/normal). This narrowed down the number of samples to 295 from 117 unique patients, with 69 males and 48 females spanning an age range from 25 years to 90 years. The average age of males is 65 years and the average age of females is 69 years. The train and test data sets were split to ensure no overlap, i.e., each patient is either present in the train or test dataset but not in both. The train data set has 233 samples from 94 unique patients and the test data set has 62 samples from 23 unique patients. 12-lead ECG and demographic information (age, race and gender) are collected for each patient. Singlelead median-filtered ECG data from V4 lead is used for this work. Fig. 2 shows an example of ECG data from V4 lead which shows a regular rhythm ECG signal and after median filtering. Median filtering suppresses noise on the ECG signal and reduces its size. The median-filtered ECG signals are directly sent as inputs to the RC without any feature extraction. This allows the RC to extract relevant information from the ECG signal directly without any loss introduced by feature extraction and also simplifies the circuit design by removing the feature extractor.

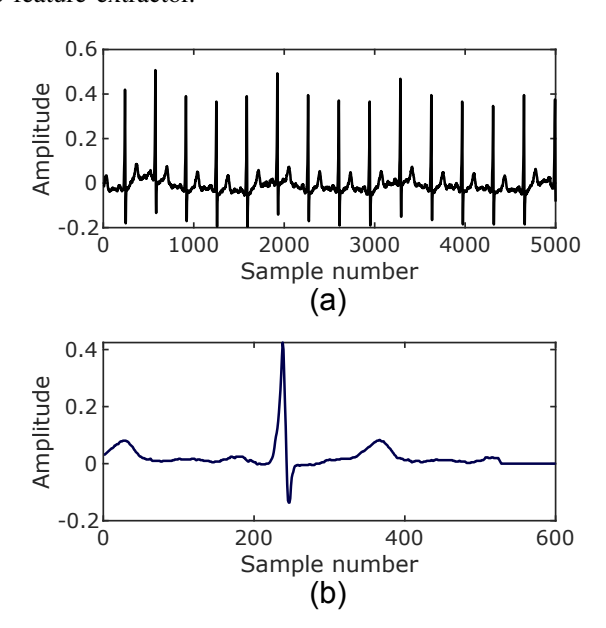


Fig. 2: Example of a) rhythm ECG signal from V4 lead; and b) ECG signal after median filtering

III. PROPOSED ARCHITECTURE

A. Overview of RC circuits

RC is a well-known computing paradigm that uses static nonlinearity to project the input signal to high-dimensional space, thus allowing easier separation of different input classes. No training is performed in the input or reservoir layers, and the weights are drawn from random distribution. Since RC uses nonlinear projection to separate data classes,

it does not need high linearity circuits which significantly reduces power consumption. RC also performs natural encoding and compression of the sensor input which reduces RF transmission packet size and power. While RC has been extensively used in the machine-learning literature, hardware implementations have been mostly on optics/photonics platform with few analog silicon implementations [3]–[6]. The works in [3]– [5] require either large capacitors to realize biological timeconstants which is energy-inefficient, or background calibration for analog delay elements or nonlinearity element. Our prior work [6] presented an on-chip analog RC that used timemultiplexing to create multiple virtual neurons from a single physical neuron without requiring large capacitors or calibration. However, the RC in [6] used continuous-time circuits which are not power efficient for bio-medical applications with slowly varying signals. The key differentiation of this work over [6] is the adoption of switched-capacitor architecture for realizing RC neurons which reduced energy consumption by $5\times$, and putting all the neurons physically on-chip.

B. Circuit design

Output of the RC with N reservoir neurons can be mathematically expressed as

$$\vec{R_k}[n] = H\left(G_i \vec{W} \times \vec{X^T} + G_f \vec{W_r} \times \vec{R_k}[n-1]\right) \tag{1}$$

where $\vec{X} = [X_1 X_2 \cdots X_D]$ is analog ECG input with D samples, \vec{W} is $N \times D$ input weight matrix, (D >> N), $\vec{W_r}$ is $N \times N$ inter-connection weight matrix for the reservoir layer, $H(\cdot)$ is nonlinear activation for RC, G_i is input scaling factor and G_f is feedback gain.

Fig. 3a) shows the schematic of the proposed switchedcapacitor RC architecture. As seen from (1), each neuron behaves as a leaky integrator which is realized by using a switched-capacitor integrator with low gain (≈ 25) as shown in Fig. 3b). Each neuron is connected to its immediate two neighboring neurons and the corresponding $\vec{W_r}$ matrix is shown in Fig. 3a). The integrator is reset if its output voltage exceeds a threshold voltage. The reservoir layer has built-in lateral inhibition which resets all three neurons in a cluster if one of the neurons is reset. This functionality is inspired by human retina in which lateral inhibition plays an important role in detecting transients, such as QRS complex in ECG signal. The feedback gain G_f and input scaling factor G_i are set by ratios of sampling capacitors C_{in} , C_{f1} and C_{f2} to the feedback capacitor C_{intg} . The number of RC neurons N, feedback gain, input scaling factor and sparsity of the interconnect matrix are set by simulating the software RC model. All the sampling capacitors C_{in} , C_{f1} and C_{f2} are set to 14.8fF each and C_{intg} is set to 44.4fF. The RC accepts median-filtered ECG signals with D = 600 samples as input and uses N = 30 neurons for encoding, i.e., the ECG data is compressed by a factor of $20\times$ by the RC. Nonlinearity of $H(\cdot)$ comes from multiple sources - a) nonlinearity of the amplifier which operates in slew mode; b) reset functionality in the integrator; c) charge injection error from the switches. In contrast to conventional analog design which requires careful matching, large area, and power to suppress mismatch and nonlinearity, the proposed analog RC neurons can be extremely small since nonlinearity due to component mismatch and biasing (such as slewing) are absorbed into the nonlinear RC kernel and leveraged for classification. The input weight matrix \vec{W} is restricted to binary '1/0' elements only and multiplication of the input samples with \vec{W} is performed off-chip to allow testing the chip with different input sample sizes D.

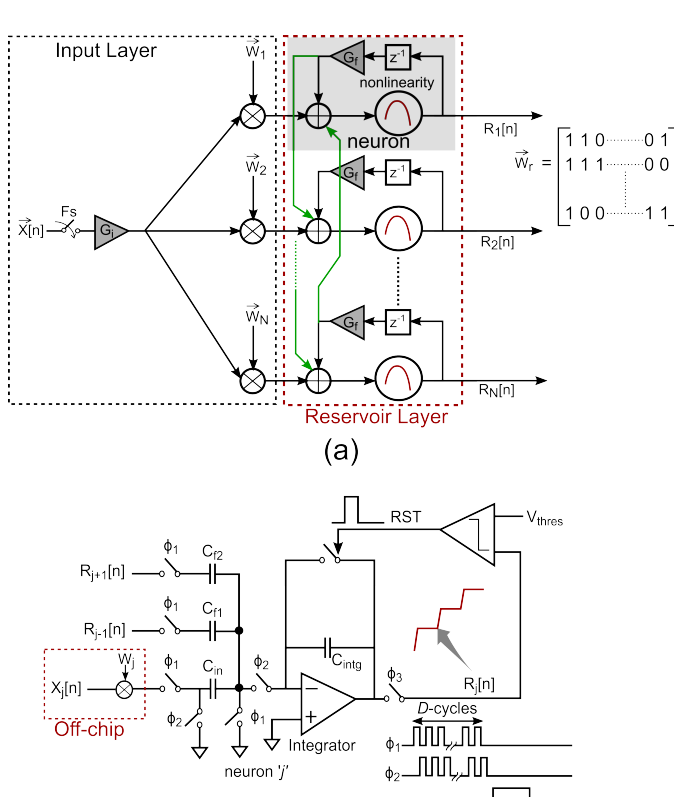


Fig. 3: Schematic of a) RC architecture; and b) single reservoir neuron

(b)

The analog RC neuron outputs are serialized and digitized using a single 10-bit successive approximation register analog-to-digital converter (SAR ADC) before they are brought off-chip. The SAR ADC uses bi-directional single-sided switching technique [7] to reduce switching energy of the ADC. Non-linearities in the ADC are amortized into the reservoir nonlinearity $H(\cdot)$ and does not require careful design unlike the ADCs used in the analog front-end circuits for digitizing sensor signals.

C. ECG and EMR Fusion

Output of the reservoir neurons are sent to a neural network for predicting AKI onset. Basic demographic information – age, race and gender of the patients are used for the EMR model. Patient race and gender information are one-hot-encoded to ensure all race and gender entries are equally weighted when applied to a neural network, while the patient ages are grouped into bins. The prediction scores from the ECG and EMR models are sent to another neural network which acts as meta-learner and performs late fusion of ECG

and EMR. In order to perform a comprehensive analysis, we evaluated three neural network models – logistic regression (LR), support vector machine (SVM) and artificial neural network (ANN). Hyper-parameters of the neural networks are optimized through grid search on training dataset, and the evaluation results on the test set are summarized in Table I. ANN performs the best for all of ECG, EMR and fusion models. For the ECG model, a 3-layer ANN is used with 60 hidden neurons in the first hidden layer, 1 hidden neuron in the second hidden layer, and 1 output neuron and tanh activation; for the EMR model, a 3-layer ANN is used with 30 hidden neurons in the first hidden layer, and 10 hidden neurons in the second hidden layer, and 1 output neuron and tanh activation; and for the fusion model a 2-layer ANN is used with 200 hidden neurons and 1 output neuron and relu activation.

TABLE I: Performance of different neural networks

	ECG	EMR	Fusion
Logistic regression	56%	56%	61%
Support vector machine	59%	56%	64%
Artificial neural network	68%	70%	76%

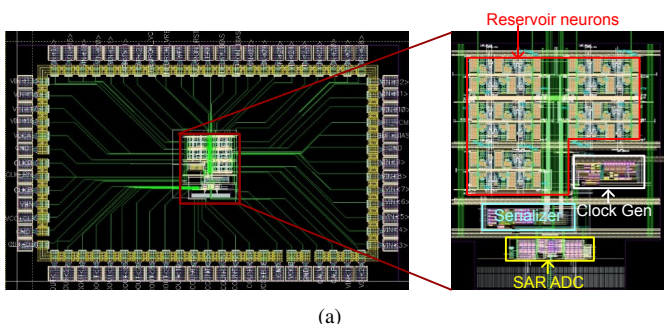
IV. MEASUREMENT RESULTS

Fig. 4a) shows the microphotograph of the test-chip in 28nm CMOS and layout view. The test-chip is fully covered with dummy metal fills to meet metal density requirements in this technology node. Additional parasitic capacitors due to the dummy metals are not an issue for this test-chip since any non-linearity introduced by these additional parasitic capacitors is amortized into the reservoir nonlinearity. The test-chip consumes $101\mu W$ from 0.9V supply while operating at 66.7 kHz and the SAR ADC operates at 2MHz. The core circuits occupy an area of $1.64 mm \times 1.04 mm$. Fig. 4b) shows the test board. The input ECG samples are applied to the test-chip using National Instruments Data Acquisition (DAQ) boxes and the chip outputs are captured by a logic analyzer.

Fig. 5 shows the confusion matrices for the ECG, EMR and fusion models. The ECG model has a low sensitivity, while the EMR model has a high sensitivity. Their fusion improves both accuracy and sensitivity metrics. The EMR model has less samples than the ECG model since the same patient has multiple ECG samples in both train and test sets. While performing fusion, the same EMR prediction score is used for all occurrences of ECG from the same patient since the demographic information is static in nature.

Table II compares this work with state-of-the-art chronic kidney diseases (CKD)/AKI detection/onset prediction tasks from ECG and EMR data. Fusion of single-lead ECG and EMR allows the proposed technique to achieve comparable or better results than state-of-the-art AI models using information from all 12-lead ECG data. Fig. 6 plots energy/inference of different bio-medical application specific integrated circuits (ASICs) with energy/inference of the proposed analog RC. The RC test-chip consumes 1.5nJ/inference which is almost 9× lower than the next best bio-medical ASIC reported in [8] which demonstrates the potential for application of the proposed RC circuit as a smart wearable.





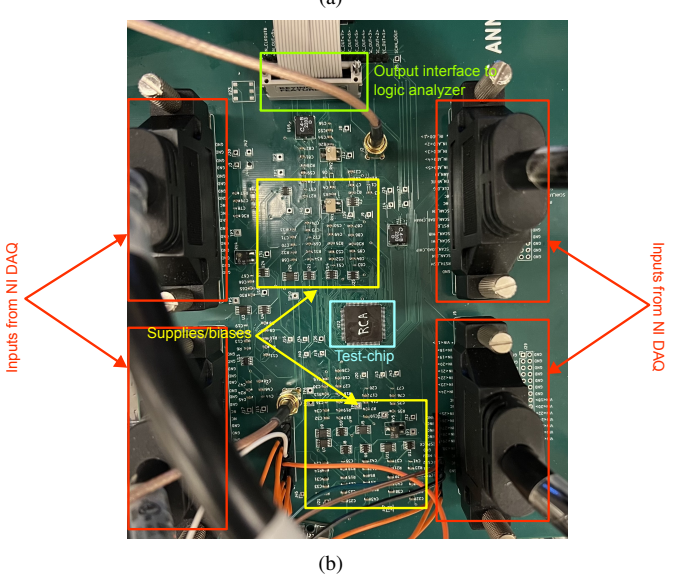


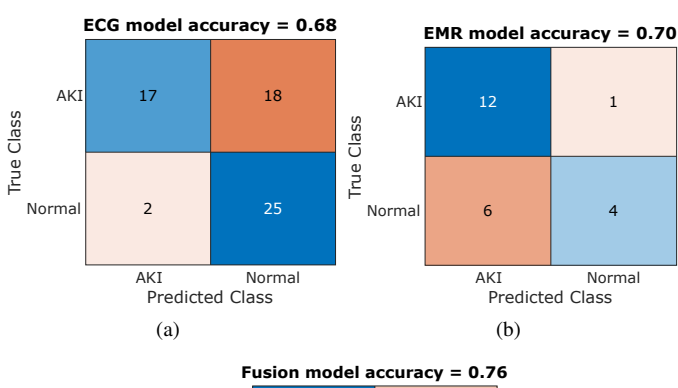
Fig. 4: a) Die photograph and layout view of the test-chip; b) picture of the test board with the chip and equipment interfaces

TABLE II: Comparison with kidney disease detection tasks

	Task	Predictor	Accuracy	AUC
[9]	CKD onset within 1 year	12-lead ECG	_	0.71
[10]	AKI onset within 2 days	EMR	55.8%	_
[11]	Renal impairment	12-lead ECG	_	0.86
This work A	AKI onset within 3-7 days	1-lead ECG+EMR	75.8%	0.76

V. CONCLUSION

This work has presented an AI-enabled fusion framework for predicting AKI recurrence 3-7 days before onset by combining single-lead ECG and demographics data. The proposed framework is evaluated on retrospective data collected from Mayo Clinic Enterprise and demonstrates the potential of athome monitoring for AKI patients using a wearable with on-



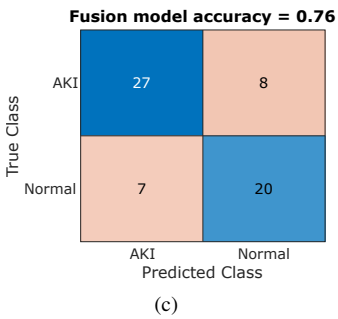


Fig. 5: Confusion matrices from a) ECG model; b) EMR model; and c) Fusion model

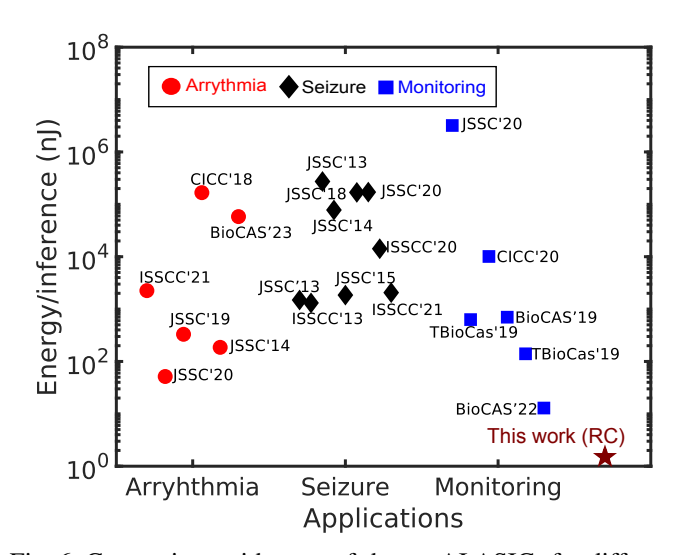


Fig. 6: Comparison with state-of-the-art AI ASICs for different bio-medical applications

device AI and smart phone.

ACKNOWLEDGMENT

This work is partially supported by National Institutes of Health under grant number R01 EB035403-02 and Alphacore Inc. under DoE grant number DE-SC0022923.

REFERENCES

- J. Vanmassenhove, R. Vanholder, and N. Lameire, "Points of concern in post acute kidney injury management," *Nephron*, vol. 138, no. 2, pp. 92–103, 2018.
- [2] M. Le Berre, E. Ressayre, A. Tallet, H. Gibbs, D. Kaplan, and M. Rose, "Conjecture on the dimensions of chaotic attractors of delayed-feedback dynamical systems," *Physical Review A*, vol. 35, no. 9, p. 4020, 1987.

- [3] F. C. Bauer, D. R. Muir, and G. Indiveri, "Real-time ultra-low power ECG anomaly detection using an event-driven neuromorphic processor," *IEEE Transactions on Biomedical Circuits and Systems*, vol. 13, no. 6, pp. 1575–1582, 2019.
- [4] K. Bai and Y. Yi, "DFR: An energy-efficient analog delay feedback reservoir computing system for brain-inspired computing," ACM Journal on Emerging Technologies in Computing Systems (JETC), vol. 14, no. 4, pp. 1–22, 2018.
- [5] Y. Chen, E. Yao, and A. Basu, "A 128-channel extreme learning machine-based neural decoder for brain machine interfaces," *IEEE transactions on biomedical circuits and systems*, vol. 10, no. 3, pp. 679–692, 2015.
- [6] S. T. Chandrasekaran, I. Banerjee, and A. Sanyal, "7.5 nJ/inference CMOS Echo State Network for Coronary Heart Disease prediction," in IEEE European Solid-State Device Research Conference (ESSDERC), 2021, pp. 103–106.
- [7] L. Chen, A. Sanyal, J. Ma, and N. Sun, "A 24-µW 11-bit 1-MS/s SAR ADC with a bidirectional single-side switching technique," in *IEEE European Solid State Circuits Conference (ESSCIRC)*, 2014, pp. 219–222.
- [8] S. Sadasivuni, S. P. Bhanushali, I. Banerjee, and A. Sanyal, "A 43.6 TOPS/W AI Classifier with Sensor Fusion for Sepsis Onset Prediction," in *IEEE Biomedical Circuits and Systems Conference (BioCAS)*, 2022, pp. 569–572.
- [9] L. Holmstrom, M. Christensen, N. Yuan, J. Weston Hughes, J. Theurer, M. Jujjavarapu, P. Fatehi, A. Kwan, R. K. Sandhu, J. Ebinger et al., "Deep learning-based electrocardiographic screening for chronic kidney disease," Communications Medicine, vol. 3, no. 1, p. 73, 2023.
- [10] N. Tomašev, X. Glorot, J. W. Rae, M. Zielinski, H. Askham, A. Saraiva, A. Mottram, C. Meyer, S. Ravuri, I. Protsyuk *et al.*, "A clinically applicable approach to continuous prediction of future acute kidney injury," *Nature*, vol. 572, no. 7767, pp. 116–119, 2019.
- [11] J.-m. Kwon, K.-H. Kim, Y.-Y. Jo, M.-S. Jung, Y.-H. Cho, J.-H. Shin, Y.-J. Lee, J.-H. Ban, S. Y. Lee, J. Park et al., "Artificial intelligence assessment for early detection and prediction of renal impairment using electrocardiography," *International Urology and Nephrology*, vol. 54, no. 10, pp. 2733–2744, 2022.